Available online at www.sciencedirect.com
SCIENCE DIRECT®
Precambrian Research 136 (2005) 353–368
Precambrian Research
www.elsevier.com/locate/precamres

Multistage magmatic and metamorphic evolution in the Southern Siberian Craton: Archean and Palaeoproterozoic zircon ages revealed by SHRIMP and TIMS

Ulrike Poller[a,*], Dmitry Gladkochub[b], Tatiana Donskaya[b], Anatoli Mazukabzov[b], Eugene Sklyarov[b], Wolfgang Todt[a]

[a] *Max-Planck-Institut für Chemie, Abt. Geochemie, Postfach 3060, D-55020 Mainz, Germany*
[b] *Institute of Earth's crust, Russian Academy of Sciences, Siberian Branch, Irkutsk, Russia*

Received 18 March 2004; accepted 17 December 2004

Abstract

This U–Pb zircon geochronological study using TIMS and SHRIMP dating reveals new insights into the magmatic and metamorphic evolution of the Siberian Craton.

Granulites, granites and one migmatite substantiate a multistage history. For the granulites an Archean protolith (3.4 Ga) is documented, followed by a first granulite formation at 2.6 Ga. In the Palaeoproterozoic a migmatisation event at 2.0 Ga and two stages of granulitisation and granite emplacement at 1.88 Ga and 1.85 Ga are detected. The latter event (1.85 Ga) is interpreted to mark the final consolidation of the Siberian Craton. Therefore this part of the craton was protected from younger overprints during the assembly of Rodinia in the Mesoproterozoic.
© 2005 Elsevier B.V. All rights reserved.

Keywords: Siberian Craton; Granulite; Zircon dating; SHRIMP

1. Introduction

Along the southern margin of the Siberian Craton there are several well-exposed salient of Precambrian basement such as the Sharizhalgai, Goloustnaja, Primorsk and Baikal block. The dominant crystalline rocks are gneisses, schists, amphibolites, granulites, migmatites and granitoids of mostly unknown age.

From the four salient sampled in this study only one, the Sharizhalgai salient, has been investigated with regard to the geochronological evolution during an earlier study. Aftalion et al. (1991) used U–Pb zircon and monazite multigrain analyses together with Rb–Sr and Sm–Nd to get the first geochronological data for southern part of the Sharizhalgai salient. Their investigations resulted e.g. in an upper intercept

* Corresponding author.
E-mail address: poller@mpch-mainz.mpg.de (U. Poller).

0301-9268/$ – see front matter © 2005 Elsevier B.V. All rights reserved.
doi:10.1016/j.precamres.2004.12.003

age of 2568 +95/−47 Ma and a lower intercept age of 1921 +195/−229 Ma for kinzingites. Aftalion et al. (1991) found rather similar ages for pyroxene bearing granodiorites (upper intercepts around 2.7 Ga, lower intercepts around 1.8 Ga).

The main aim of our study was to increase the geochronological knowledge along the southern margin of the Siberian Craton in order to better reconstruct the magmatic and metamorphic evolution of the whole region. One question in this context was whether this area could give new information on the role of Siberia during the Rodinia supercontinent amalgamation.

The age determinations were done using U–Pb single zircon dating by thermal ion mass spectrometry (TIMS) for the migmatite and some of the granites and by SHRIMP spot analyses on cathodoluminescence pre-investigated zircons.

2. Geological introduction

In fact the southern part of the Siberian Craton (Fig. 1A) is composed of numerous blocks (units) different in age and composition, which generally correspond to the southern margins of Tungus (West) and Magan (East) terranes and Akitkan belt (according to scheme Rosen et al., 1994).

All of these units are characterized by prevailing of Archean or Palaeoproterozoic continental crust and can be described as exposed fragments (salient) of basement complexes. In present time the main part of the Siberian Craton is covered by Precambrian and Paleozoic sediments and only some rather small uncovered parts (salient) remain available for studying and sampling.

The studies were focused on Sharizhalgai (ShS), Goloustnaja (GS), Primorsk (PS) and North-Baikal (BS) salient (Fig. 1B).

The Sharizhalgai salient is the southern termination of the Tungus terrane. At the west it borders with Angara belt, which surrounds the southern and western margins of this terrane. Goloustnaja and Primorsk salient belong to southern part of the Magan terrane. The North Baikal salient is located within the Akitkan belt (according Rosen et al., 1994). In general this belt is described as suture zone between the Magan and Aldan terranes (Fig. 1A and B).

The Sharizhalgai salient is the mostly southern part of the craton. This well exposed salient could be traced in S-E direction up to 400 km from Urik River in the West to the southern part of Baikal Lake. The metamorphic complexes of this salient include gneisses, schists, amphibolites and granulites (acid and mafic in composition). Among these rocks occur beds of marbles and sillimanite-rich rocks. On the base of geochronological data reported by Aftalion et al. (1991) for the Sharizhalgai salient two age groups were distinguished: Upper Archean and Palaeoproterozoic ages. The metamorphic complexes of the Sharizhalgai salient is intruded by Upper Archean (2.53 Ga) Kitoy granites (Gladkochub et al., 2005), Palaeoproterozoic (1.86 Ga) Sayan and Shumikha granites (Donskaya et al., 2002; Levitskii et al., 2002) and Neoproterozoic doleritic dikes (Gladkochub et al., 2003).

The Goloustnaja salient is exposed at the Western coast-line (shore) of Lake Baikal. The salient consists of migmatite, gneiss and amphibolite. This metamorphic basement complex is intruded by the 1.86 Ga Primorsk rapakivi-like granite (Donskaya et al., 2003).

The major part of the Primorsk salient is composed of Primorsk rapakivi-like granite. Schists and acidic granulites represent rare relicts of metamorphic complexes.

The main volume of the Baikal salient (North-Baikal Ridge) is built by the volcanic and volcanic-sedimentary sequence of the Akitkan series (1.87–1.85 Ga) (Larin et al., 2003) and Irel granites.

3. Sample description

For this study one migmatite, six granulites and three granites from five different locations of the southern part of the Siberian Craton were sampled. The locations (see Fig. 1B) cover a distance of about 500 km along the southern marginal area of the craton fitting to four of the above-mentioned salient.

3.1. The Sharizhalgai salient

The western most outcrops are situated at the Kitoy River area, approximately 150 km west of Irkutsk (Fig. 1B). Three localities were sampled at this area.

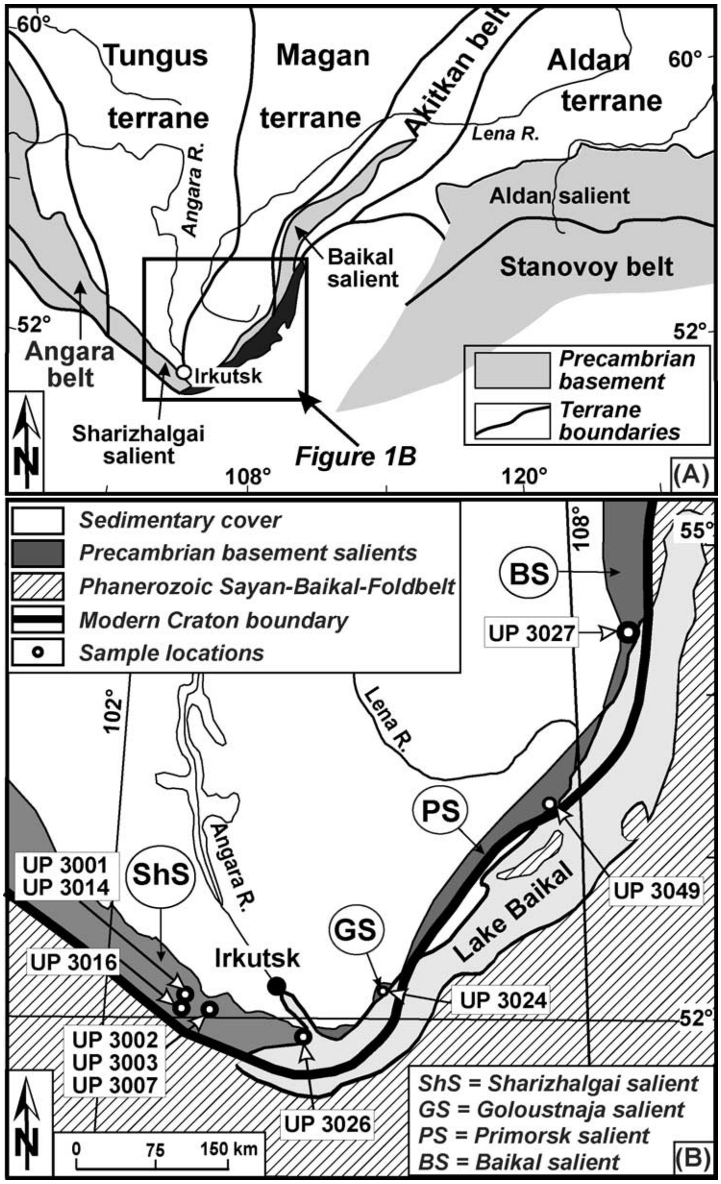

Fig. 1. (A) Scheme of terranes of southern part of the Siberian Craton (modified after Rosen et al., 1994). (B) Scheme of main units of the southern part of the Siberian Craton and sample locations.

The first outcrop (52°15.30′N, 102°48.75′E) occurs on the left shore of the Kitoy River. This outcrop covers about 2 km along the river and exhibits gneisses, granulites and intercalated lenses of marbles. The metamorphic basement complex is intruded by granitic bodies and Neoproterozoic doleritic dikes (Gladkochub et al., 2003). At this outcrop the granite (UP 3001) and the granulite (UP 3014) have been collected (Fig. 1B).

The next outcrop allocated at the right side of the Kitoy River (52°07.01′N, 102°56.51′E) consists of garnet-bearing and garnet-free granulites, metabasites, and granitoids. The syenite (UP 3002) and the

Table 1
U–Pb zircon SHRIMP data

Grain spot	CL	U (ppm)	Th (ppm)	Th/U	Pb* (ppm)	Radiogenic ratios								Age (Ma)					
						$^{204}Pb/^{206}Pb$	$^{206}Pb/^{238}U$	±	$^{207}Pb/^{235}U$	±	$^{207}Pb/^{206}Pb$	±	ρ	$^{206}Pb/^{238}U$	±	$^{207}Pb/^{206}Pb$	±	% Disc	Fig.
UP 3001 Kitoy Granite ($n = 8$)																			
35.1	dr	758	399	0.53	225	0.000202	0.3444	71	5.422	129	0.1142	14	0.860	1908	34	1867	22	−2	3e
35.2	gm	712	298	0.42	208	0.000019	0.3405	71	5.370	116	0.1144	6	0.978	1889	34	1870	8	−1	3e
36.1	dr	1085	246	0.23	307	0.000009	0.3294	67	5.185	106	0.1142	4	0.983	1836	32	1867	6	2	3e
39.1	gr	551	300	0.54	170	0.000080	0.3587	73	5.610	120	0.1134	8	0.950	1976	35	1855	12	−7	3e
39.2	dc	692	353	0.51	209	0.000016	0.3521	73	5.558	116	0.1145	6	0.976	1944	34	1872	8	−4	3e
40.1	dc	1428	727	0.51	442	0.000008	0.3598	73	5.657	114	0.1140	4	0.987	1981	34	1865	6	−6	3e
43.1	bc	351	196	0.56	101	0.000023	0.3352	71	5.274	116	0.1141	8	0.950	1864	34	1866	12	0	3e
43.2	dr	663	571	0.86	189	0.000072	0.3322	67	5.222	110	0.1140	6	0.962	1849	33	1864	10	1	3e
UP 3002 Kitoy Syenite ($n = 11$)																			
19.1	br	267	134	0.50	77	0.000029	0.3352	71	5.250	118	0.1136	8	0.946	1864	34	1858	14	0	3f
20.1	dr	455	478	1.05	131	0.000020	0.3357	92	5.299	153	0.1145	10	0.959	1866	45	1872	16	0	3f
22.1	gm	402	348	0.87	115	0.000002	0.3323	71	5.231	114	0.1142	8	0.961	1850	34	1867	12	1	3f
23.1	br	140	96	0.69	41	0.000089	0.3385	82	5.319	143	0.1140	12	0.912	1880	40	1863	20	−1	3f
25.1	dr	732	559	0.76	213	0.000001	0.3385	74	5.357	122	0.1148	6	0.980	1879	36	1876	8	0	3f
27.1	dr	407	363	0.89	117	0.000040	0.3351	69	5.270	116	0.1141	8	0.952	1863	34	1865	12	0	3f
27.2	dr	330	289	0.88	95	0.000008	0.3348	102	5.249	174	0.1137	16	0.912	1862	49	1859	26	0	3f
28.1	dr	499	389	0.78	147	0.000012	0.3426	73	5.434	122	0.1150	8	0.942	1899	35	1880	14	−1	3f
29.1	dr	267	211	0.79	78	0.000017	0.3407	73	5.344	122	0.1138	10	0.928	1890	35	1860	16	−2	3f
29.2	br	194	132	0.68	57	0.000046	0.3419	74	5.355	127	0.1136	12	0.911	1896	36	1858	18	−2	3f
31.2	br	196	143	0.73	57	0.000069	0.3357	80	5.262	141	0.1137	14	0.887	1866	39	1859	22	0	3f
UP 3003 Kitoy Granulite ($n = 10$)																			
27.1	gr	367	72	0.20	97	0.000030	0.3086	65	4.868	126	0.1144	18	0.820	1734	32	1871	27	7	2b
30.1	gm	445	389	0.87	184	0.000019	0.4815	101	11.173	246	0.1683	12	0.954	2534	44	2541	12	0	2a
31.1	gm	424	411	0.97	179	0.000010	0.4922	103	11.822	253	0.1742	8	0.976	2580	45	2599	8	1	2a
39.1	dc	1390	256	0.18	563	0.000006	0.4712	104	11.144	252	0.1715	8	0.974	2489	46	2573	8	3	2a
48.2	dr	3593	1622	0.45	675	0.000113	0.2183	44	3.208	69	0.1066	8	0.947	1273	23	1742	12	27	2b
50.1	dr	333	176	0.53	95	0.000001	0.3308	71	5.241	118	0.1149	8	0.947	1842	34	1878	14	2	2b
50.2	gm	843	170	0.20	362	0.000012	0.4999	115	11.481	288	0.1666	18	0.915	2613	49	2524	18	−4	2a
54.1	gr	303	161	0.53	91	0.000019	0.3480	74	5.486	124	0.1143	8	0.950	1925	36	1869	12	−3	2b
54.2	dc	460	429	0.93	126	0.000009	0.3197	66	5.056	109	0.1147	6	0.961	1788	32	1875	10	5	2b
58.1	gm	300	271	0.90	132	0.000015	0.5111	122	12.008	293	0.1704	8	0.978	2661	52	2562	8	−4	2a

UP 3007 Kitoy Granulite ($n = 36$)																		
22.1	gr	441	107	0.24	146	0.000002	0.3853	153	8.580	351	0.1615	8	0.975	2101	37	2471	8	15	2c
23.1	dr	661	207	0.31	229	0.000006	0.4040	163	9.200	380	0.1652	8	0.971	2187	38	2509	8	13	2c
25.1	br	263	49	0.19	72	0.000031	0.3195	133	5.815	261	0.1320	10	0.939	1787	34	2125	14	16	2c
25.2	dm	1009	98	0.10	354	0.000003	0.4088	161	9.255	366	0.1642	4	0.989	2210	37	2499	6	12	2c
25.3	dm	676	220	0.32	260	0.000009	0.4485	208	10.648	498	0.1722	6	0.990	2389	47	2579	6	7	2c
31.2	bc	112	64	0.57	54	0.000016	0.5583	300	22.130	1319	0.2875	24	0.948	2859	58	3404	14	16	2d
32.2	gr	584	173	0.30	229	0.000005	0.4567	200	10.778	480	0.1712	6	0.986	2425	45	2569	6	6	2c
37.2	gr	446	98	0.22	114	0.000014	0.2979	155	5.014	312	0.1221	22	0.839	1681	39	1987	31	15	2c
38.1	gr	784	151	0.19	284	0.000002	0.4214	161	9.792	386	0.1685	8	0.984	2267	45	2543	8	11	2c
39.1	br	196	52	0.27	54	0.000001	0.3190	159	5.613	308	0.1276	16	0.909	1785	40	2066	22	14	2c
39.2	br	200	44	0.22	54	0.000137	0.3125	135	5.880	357	0.1364	30	0.713	1753	34	2182	37	20	2c
39.3	dc	486	153	0.31	144	0.000019	0.3458	92	7.726	235	0.1620	22	0.894	1915	43	2477	22	23	2d
42.1	dr	455	130	0.29	184	0.000008	0.4713	194	11.220	476	0.1726	10	0.971	2489	43	2583	8	4	2c
42.2	dc	781	228	0.29	311	0.000003	0.4636	265	10.931	758	0.1710	10	0.966	2456	46	2567	10	4	2c, d
43.2	gr	336	63	0.19	116	0.000003	0.4004	167	8.991	386	0.1629	10	0.965	2171	39	2486	10	13	2c
44.1	bc	122	110	0.91	57	0.000024	0.5442	220	19.677	876	0.2622	20	0.956	2801	53	3260	12	14	2d
44.2	dr	340	56	0.17	113	0.000007	0.3884	163	8.549	372	0.1596	10	0.956	2115	38	2452	12	14	2c
50.1	br	528	153	0.29	171	0.000192	0.3771	151	7.564	335	0.1455	14	0.910	2063	36	2293	16	10	2c
50.2	dr	1301	377	0.29	456	0.000001	0.4082	161	9.236	376	0.1641	10	0.961	2207	37	2498	10	12	2c
52.1	gr	461	125	0.27	186	0.000015	0.4692	206	11.062	499	0.1710	10	0.966	2480	46	2567	10	3	2c
56.2	bc	135	56	0.41	59	0.000039	0.5073	280	15.559	590	0.2225	42	0.784	2645	50	2999	29	12	2d
56.3	bc	149	61	0.41	72	0.000018	0.5593	257	18.270	1396	0.2369	54	0.709	2864	52	3099	35	8	2d
61.1	br	501	132	0.26	210	0.000030	0.4882	196	11.479	470	0.1705	8	0.979	2563	43	2563	8	0	2c
61.2	br	389	99	0.25	165	0.000019	0.4939	200	11.776	498	0.1729	10	0.962	2587	44	2586	10	0	2c
61.3	dr	681	174	0.26	281	0.000015	0.4792	190	11.365	468	0.1720	10	0.966	2524	42	2577	10	2	2c
62.2	bc	187	208	1.11	77	0.000032	0.4760	337	12.636	1147	0.1925	26	0.878	2510	52	2764	22	9	2d
62.3	gr	578	178	0.31	221	0.000001	0.4451	182	10.195	465	0.1661	18	0.893	2374	41	2519	18	6	2c
UP 3007 Kitoy Granulite ($n = 36$)																			
65.1	gr	240	97	0.41	97	0.000042	0.4719	200	11.046	511	0.1698	16	0.919	2492	45	2556	16	2	2c
69.3	gr	480	124	0.26	204	0.000008	0.4949	204	11.855	527	0.1737	16	0.927	2592	45	2594	14	0	2c
80.1	dr	672	202	0.30	254	0.000010	0.4407	186	10.260	447	0.1689	10	0.965	2354	42	2546	10	8	2c
99.1	bc	100	61	0.61	47	0.000150	0.5424	329	16.370	1027	0.2189	30	0.979	2794	139	2972	20	6	2d
100.1	dc	1509	417	0.28	630	0.000009	0.4860	190	11.800	463	0.1761	8	0.996	2553	84	2617	6	2	2c, d
101.1	dc	764	344	0.45	376	0.000094	0.5718	235	16.530	843	0.2097	62	0.800	2915	95	2903	49	0	2d
102.1	gm	349	109	0.31	145	0.000004	0.4823	208	11.050	498	0.1661	24	0.957	2537	90	2519	22	−1	2c
103.1	dc	1382	98	0.07	424	0.000023	0.3567	147	6.080	251	0.1236	8	0.988	1967	68	2009	12	2	2d
105.1	dc	3660	860	0.23	1632	0.000004	0.5191	204	14.220	556	0.1987	8	0.995	2695	88	2815	6	4	2d

Table 1 (*Continued*)

Grain spot	CL	U (ppm)	Th (ppm)	Th/U	Pb* (ppm)	Radiogenic ratios								Age (Ma)					
						$^{204}Pb/^{206}Pb$	$^{206}Pb/^{238}U$	±	$^{207}Pb/^{235}U$	±	$^{207}Pb/^{206}Pb$	±	ρ	$^{206}Pb/^{238}U$	±	$^{207}Pb/^{206}Pb$	±	% Disc	Fig.
UP 3014 Kitoy Granulite (*n* = 6)																			
9.1	gr	249	64	0.26	71	0.000120	0.3319	143	5.192	234	0.1135	18	0.931	1847	68	1856	29	0	2e
11.1	gr	329	89	0.27	95	0.000048	0.3343	138	5.228	225	0.1134	14	0.962	1859	66	1855	22	0	2e
12.1	gr	676	266	0.39	190	0.000064	0.3275	135	5.120	211	0.1134	10	0.978	1827	64	1854	16	2	2e
14.1	gm	253	72	0.28	72	0.000120	0.3324	137	5.174	223	0.1129	18	0.935	1850	66	1846	27	0	2e
14.2	gr	637	176	0.28	183	0.000073	0.3334	137	5.272	217	0.1147	12	0.974	1855	65	1875	18	1	2e
17.1	gr	465	109	0.23	132	0.000045	0.3301	136	5.140	211	0.1129	12	0.973	1839	65	1847	18	0	2e
UP 3016 Kitoy mafic Granulite (*n* = 4)																			
1.1	dc	894	315	0.35	224	0.000150	0.2923	17	4.776	58	0.1185	22	0.810	1644	34	1934	31	18	no
1.2	dr	833	239	0.29	172	0.000220	0.2410	19	3.711	84	0.1117	16	0.851	1383	29	1827	26	32	no
6.1	dr	2489	385	0.15	1087	0.000050	0.5111	30	12.012	71	0.1705	6	0.989	2647	50	2562	6	−3	no
7.1	gr	235	41	0.17	66	0.000250	0.3286	38	5.097	130	0.1125	28	0.738	1821	41	1840	43	1	no
UP 3024 Goloustnaja Migmatite (*n* = 9)																			
27.1	dr	726	184	0.25	174	0.000110	0.2790	112	4.488	186	0.1167	12	0.974	1586	57	1906	18	20	3c
32.1	dr	697	156	0.22	167	0.000140	0.2781	112	4.480	187	0.1168	14	0.965	1582	56	1908	20	21	3c
37.1	dr	823	238	0.29	187	0.000430	0.2628	107	4.181	190	0.1154	24	0.896	1504	55	1886	37	25	3c
39.1	dr	563	171	0.30	158	0.000140	0.3253	131	5.459	228	0.1217	14	0.964	1816	64	1981	20	9	3c
42.1	dr	777	213	0.27	160	0.000420	0.2373	96	3.673	163	0.1123	20	0.909	1373	50	1836	33	34	3c
43.1	dr	736	208	0.28	186	0.000088	0.2939	118	4.786	198	0.1181	12	0.974	1661	59	1928	18	16	3c
44.1	dr	455	158	0.35	142	0.000490	0.3602	146	6.106	286	0.1229	30	0.865	1983	69	1999	41	1	3c
44.2	dr	444	80	0.18	139	0.001000	0.3590	150	6.171	333	0.1247	42	0.774	1978	71	2024	61	2	3c
45.1	dr	778	296	0.38	175	0.000087	0.2613	112	4.121	180	0.1144	12	0.979	1496	57	1870	16	25	3c
UP 3026 South Baikal Granulite (*n* = 24)																			
30.1	dm	567	136	0.24	168	0.000032	0.3444	80	5.440	139	0.1146	14	0.901	1908	39	1873	22	−2	3a
31.1	dc	46	104	2.26	13	0.000400	0.3305	149	5.230	327	0.1148	49	0.727	1841	74	1877	78	2	3a
34.1	dc	221	218	0.99	123	0.000058	0.6488	267	24.490	1007	0.2737	22	0.985	3224	104	3327	12	3	3a
35.1	br	87	142	1.63	25	0.000330	0.3376	139	5.220	276	0.1121	37	0.773	1875	67	1834	61	−2	3a
35.2	dc	912	46	0.05	292	0.000048	0.3727	88	6.990	178	0.1360	16	0.898	2042	41	2176	20	7	3a
36.1	dc	343	539	1.57	192	0.000250	0.6472	267	23.280	1004	0.2609	35	0.954	3217	103	3252	20	1	3a
37.1	dc	320	173	0.54	175	0.000066	0.6333	272	22.590	974	0.2587	16	0.989	3163	106	3239	10	2	3a
37.2	br	42	71	1.69	12	0.000450	0.3271	155	5.150	333	0.1142	51	0.710	1824	73	1867	82	2	3a
38.1	dc	819	393	0.48	452	0.000008	0.6418	265	24.600	1013	0.2779	12	0.995	3196	103	3351	6	5	3a
39.1	br	61	96	1.57	19	0.000360	0.3584	120	6.920	339	0.1401	53	0.670	1975	56	2228	63	13	3a
39.2	dc	539	536	0.99	316	0.000001	0.6834	174	27.030	741	0.2869	18	0.983	3357	69	3401	8	1	3a

40.1	br	161	120	0.75	47	0.000001	0.3404	114	5.290	198	0.1128	20	0.871	1889	53	1845	33	−2	3a
40.2	dc	2140	1662	0.78	1212	0.000009	0.6591	155	24.330	572	0.2677	6	0.994	3264	58	3293	4	1	3a
41.1	br	134	219	1.63	39	0.000300	0.3403	94	5.330	210	0.1136	31	0.718	1888	46	1857	49	−2	3a
41.2	gr	409	636	1.56	120	0.000048	0.3409	86	5.350	147	0.1138	14	0.907	1891	40	1861	22	−2	3a
45.1	dc	96	154	1.60	58	0.000160	0.6972	300	28.090	1226	0.2922	35	0.965	3410	113	3429	18	1	3a
46.1	dc	941	462	0.49	541	0.000019	0.6686	263	26.840	1105	0.2912	24	0.978	3300	104	3424	14	4	3a
46.2	dc	807	163	0.20	423	0.000030	0.6097	251	21.970	904	0.2613	20	0.984	3069	101	3255	12	6	3a
48.1	gr	568	381	0.67	171	0.000060	0.3492	88	5.550	163	0.1153	14	0.896	1931	43	1884	24	−2	3a
49.1	dc	539	205	0.38	172	0.000053	0.3711	161	7.540	429	0.1473	55	0.745	2035	74	2315	65	14	3a
49.2	gr	63	126	2.00	18	0.000150	0.3272	167	5.110	290	0.1133	31	0.871	1825	80	1853	51	2	3a
52.1	gm	1243	921	0.74	353	0.000016	0.3307	129	5.220	216	0.1145	6	0.990	1842	64	1872	10	2	3a
52.2	br	46	104	2.26	13	0.000400	0.3305	149	5.230	327	0.1148	49	0.727	1841	74	1877	78	2	3a
53.1	dc	266	213	0.80	151	0.000053	0.6602	272	25.500	1051	0.2802	22	0.984	3268	105	3364	12	3	3a
UP 3027 Akitkan Granite (*n* = 8)																			
6.1	gr	84	37	0.44	24	0.000057	0.3275	104	5.1468	188	0.1148	20	0.863	1826	50	1864	33	2	3d
7.1	dc	273	97	0.36	50	0.003213	0.2009	67	3.1909	436	0.1587	70	0.243	1180	36	1883	237	38	3d
8.1	dc	440	208	0.47	121	0.000040	0.3194	92	5.0361	152	0.1149	8	0.963	1787	46	1870	14	5	3d
8.2	gr	107	60	0.56	30	0.000116	0.3288	102	5.1460	185	0.1151	18	0.862	1832	50	1857	33	1	3d
12.1	gr	91	45	0.49	23	0.000609	0.2881	100	4.4173	220	0.1195	20	0.692	1632	50	1819	65	11	3d
12.2	gr	319	132	0.41	37	0.001119	0.1311	39	1.9624	112	0.1238	16	0.523	794	22	1775	90	57	3d
13.1	dc	175	82	0.47	50	0.000139	0.3296	100	5.1233	172	0.1146	14	0.898	1837	48	1844	27	0	3d
13.2	br	86	39	0.45	24	0.000123	0.3282	104	5.1695	193	0.1159	20	0.845	1830	50	1868	35	2	3d
UP 3049 Kaltigey Granulite (*n* = 10)																			
9.1	bc	338	178	0.53	97	0.000048	0.3324	98	5.2843	166	0.1160	12	0.936	1850	47	1885	20	2	3b
12.1	bc	184	87	0.47	53	0.000040	0.3337	100	5.3205	171	0.1162	12	0.930	1857	48	1890	22	2	3b
12.2	dr	2375	69	0.03	681	0.000008	0.3338	96	5.2585	151	0.1144	4	0.994	1857	46	1868	6	1	3b
15.1	bc	326	170	0.52	95	0.000045	0.3372	102	5.3774	170	0.1162	10	0.956	1873	49	1890	18	1	3b
16.2	gr	271	117	0.43	80	0.000044	0.3417	100	5.4276	171	0.1158	12	0.935	1895	48	1883	20	−1	3b
17.1	dc	631	404	0.64	184	0.000025	0.3382	98	5.3654	161	0.1154	10	0.964	1878	47	1881	14	0	3b
17.2	dr	3044	120	0.04	896	0.000007	0.3424	98	5.4314	158	0.1151	4	0.995	1898	47	1881	6	−1	3b
18.1	gr	339	178	0.53	98	0.000078	0.3360	98	5.3510	164	0.1166	10	0.954	1867	47	1888	16	1	3b
18.2	dr	2127	87	0.04	623	0.000012	0.3412	98	5.3930	157	0.1148	4	0.993	1892	48	1874	6	−1	3b
19.2	br	373	188	0.50	109	0.000043	0.3398	100	5.4100	164	0.1161	8	0.962	1886	48	1887	16	0	3b

Cathodoluminescence features: dr, dark rim; gr, grey rim; br, bright rim; dc, dark center (core); bc, bright center (core); dm, dark middle area; gm, grey middle area.
For % Disc, 0% denotes a concordant analysis.
All errors refer to 95% confidence level.

granulites (UP 3003, UP 3007) were sampled from this site (Fig. 1B).

The third outcrop spreads along the left shore of the Holomha River (left tributary of the Kitoy River, at 52°11.74′N, 102°44.95′E). Amphibolites, gneisses, granulites and granites occur within this outcrop. From this outcrop the granulite (UP 3016) was taken for geochronological studies (Fig. 1B).

The granitoid samples UP 3001 and UP 3002 were first dated by single zircon U–Pb TIMS analyses (Poller et al., 2004), which are included into this study (Table 1) with new additional SHRIMP zircon ages for direct discussion with the granulite results of Kitoy area.

The Kitoy granulites differ in their geochemical and mineralogical composition. Whereas the most acidic granulite sample UP 3007 has a SiO_2 content of 72.0 wt.% the more intermediate granulite UP 3003 has only 60.8 wt.% SiO_2. Both samples bear biotite as minor mafic mineral beside orthopyroxene. Additionally granulite UP 3003 shows minor amounts of amphibole and clinopyroxene, whereas in the acidic granulite UP 3007 garnet and cordierite occur.

The samples UP 3014 and UP 3016 are rather mafic granulites. UP 3014 has only 45.89 wt.% SiO_2 and combines orthopyroxene, clinopyroxene and sphene. The second two-pyroxene granulite from Kitoy area, UP 3016 (46.4 wt.% SiO_2) contained only very few zircons (see Table 2) and it seems to be the same type of granulite as UP 3014.

The most southerly outcrop is situated on the southern shoreline of Lake Baikal (South-Baikal area) next to the old Transsiberian railway (51°47.652′N, 104°36.422′E) at the same locality Aftalion et al. (1991) used for their study. The outcrop composed of granulites, gneisses, migmatites, granitoids and dolerite dikes. At this locality granulite UP 3026 was taken (Fig. 1B). The sample contains two pyroxenes (Opx and Cpx) and apatite and has 58.77 wt.% SiO_2.

3.2. The Goloustnaja salient

Within the Goloustnaja salient the outcrop exposed on the shore of Lake Baikal at 52°04.932′N, 105°30.434′E was studied (Fig. 1B). At this outcrop occur gneisses, migmatites, amphibolites and granites. One migmatite sample (UP 3024) was collected from this outcrop. The sample (66.69 wt.% SiO_2) bears amphibole together with biotite and is rather rich in primary apatite. The zircons of this sample are magmatically zoned and dotted with up to 20 μm sized apatites, which often lower the measured $^{206}Pb/^{204}Pb$ ratios.

3.3. The Primorsk salient

Within the Primorsk salient the outcrop exposed at the Kaltigey Cape at the shore of Lake Baikal (53°30.622′N, 107°32.038′E) was investigated (Fig. 1B). The outcrop is composed of garnet-bearing granulites that are intruded by dolerite dikes. The

Table 2
U–Pb zircon data (TIMS)

Sample	Method	Measured atomic ratio[a]					Radiogenic atomic ratios[b]				Age (Ma)[b]			
		U_{tot}/Pb[a]	$^{206}Pb/^{204}Pb$	2σ m	$^{206}Pb/^{238}U$	2σ m	$^{207}Pb/^{235}U$	2σ m	$^{206}Pb/^{235}U$	2σ m	$^{206}Pb/^{238}U$	2σ m	Error correlation	Fig.
UP 3024, Goloustnaja migmatite														
3024-A	V.D.	3.25	2050	139	0.2601	16	4.261	50	0.11884	69	1490.2	8.4	0.73	3c
3024-C	V.D.	3.72	571	13	0.2277	26	3.711	70	0.11818	122	1322.6	13.5	0.72	3c
3024-E	V.D.	4.00	978	18	0.2115	16	3.342	39	0.11458	61	1236.9	8.6	0.81	3c
3024-F	V.D.	3.30	1085	24	0.2555	15	4.188	44	0.11889	67	1466.6	7.6	0.70	3c
3024-G1	V.D.	3.30	1518	48	0.2544	80	4.187	163	0.11938	135	1461.0	41	0.94	3c
3024-I	V.D.	4.17	449	3	0.2010	10	3.076	56	0.11096	169	1180.9	5.4	0.27	3c
3024-J	V.D.	3.59	870	51	0.2329	23	3.748	73	0.11673	128	1349.6	12	0.65	3c
3024-L	V.D.	4.29	426	4	0.1968	11	3.112	32	0.11467	84	1158.3	5.7	0.57	3c

V.D.: vapour digestion single zircon dating.
2σ m errors refer to the 2σ deviation of the weighted mean of 2–6 blocks.
[a] Corrected for fractionation, spike.
[b] Corrected for blank, spike and common Pb.

sampled acidic granulite UP 3049 has 77.83 wt.% SiO_2 is very garnet rich and again biotite is the major mafic mineral.

3.4. The Baikal salient

The most northern sample location (Fig. 1B) at 54°24.822′N, 108°29.581′E is part of the Akitkan belt. The studied outcrop consists of mainly granites and co-magmatic volcanics. At a cliff situated near an old mining site the granite UP 3027 (73.03 wt.% SiO_2) was sampled for geochronology. Besides plagioclase, large K-feldspars with perthitic structures are visible in thin section. The biotites show smooth regulation.

4. Analytical techniques

Zircons have been dated by SHRIMP at ANU in Canberra and Curtin University in Perth using SHRIMP RG and SHRIMP II, respectively. Additional TIMS dating was done using conventional isotope dilution techniques on single grains at the Max-Planck-Institut für Chemie in Mainz.

After crushing, the zircons were separated using standard Wilfley table, magnetic separation, and heavy liquids (Diiodomethan). Suitable zircons were selected under binocular microscope. All analysed zircons were controlled by cathodoluminescence (CL) imaging (Poller, 2000) and only inclusion free and crack free zircons or zircon areas were analysed. However, for zircons from migmatite UP 3024 apatite inclusions could not be avoided completely.

Zircons were placed in a 1-inch resin mount together with the appropriate standards for the SHRIMP. The mounts were polished and all zircons were exposed about in their mid area. After coating with carbon, secondary electron (SE) and cathodo luminescence (CL) imaging was performed using a field emission scanning electron microscope LEO 1530 (MPI Mainz, Kosmochemie).

4.1. Thermal ionisation mass spectrometer (TIMS) isotope dilution U–Pb analyses

For the TIMS dating single zircons were selected from the CL mount and dissolved in a modified Krogh bomb (Krogh, 1973) together with a $^{205}Pb/^{233}U$ spike. No chemical separation was used; instead the dissolved zircons were loaded directly onto a Re filament with Si-Gel. The Pb isotopic ratios were measured first using a SEM on a modified Finnigan MAT 261 mass spectrometer at around 1350 °C. After raising the temperature up to 1450 °C the U isotopes were analysed as UO_2^+. Pb compositions were corrected for mass discrimination as determined by analyses of NBS SRM 982 (equal-atom) Pb (Todt et al., 1996) and monitored by analyses at the beginning and end of each carrousel. Uranium fractionation was monitored by analyses of NBS SRM U500. Uncertainties in Pb/U ratios due to uncertainties in fractionation and low intensities for single zircons were in the range of 1%. Radiogenic ^{208}Pb, ^{207}Pb, and ^{206}Pb were corrected for the laboratory blank monitored using the center hole of the dissolution bomb, and for initial common Pb using the measured composition of cogenetic feldspars.

4.2. SHRIMP U–Pb analyses

For the SHRIMP (Sensitive High Resolution Ion Microprobe) the mounts were polished and gold coated after CL imaging. Analyses were done on areas carefully selected by transmitted light, SE and CL images. Spot sizes were between 20 and 25 μm. The standards were SL13 and FC-1 in Canberra and SL13 and CZ3 in Perth. Operating procedures for U, Th, and Pb isotopic measurements are based on those described by Compston et al. (1984) and Williams (1998).

Each spot was mass scanned seven times and standards were analysed after every group of 3 sample spots. The raw data were corrected for non-radiogenic Pb using ^{204}Pb as a monitor and the composition of Pb measured on TIMS in Mainz on cogenetic feldspars.

For ratio calculation the SQUID program, version 1.02, was used (Ludwig, 2001).

All data (TIMS and SHRIMP) were finally calculated using Isoplot, version 2.1, (Ludwig, 1999).

All results are summarised in Tables 1 and 2 and are shown in concordia plots (Figs. 2 and 3) with 95% confidence level (2 sigma errors).

5. Results

5.1. The Sharizhalgai salient: Kitoy Granulites (UP3003, UP3007, UP3014, UP 3016)

The Kitoy granulite UP 3003 was dated using the SHRIMP RG in Canberra. Ten analyses of several grains resulted in two age groups.

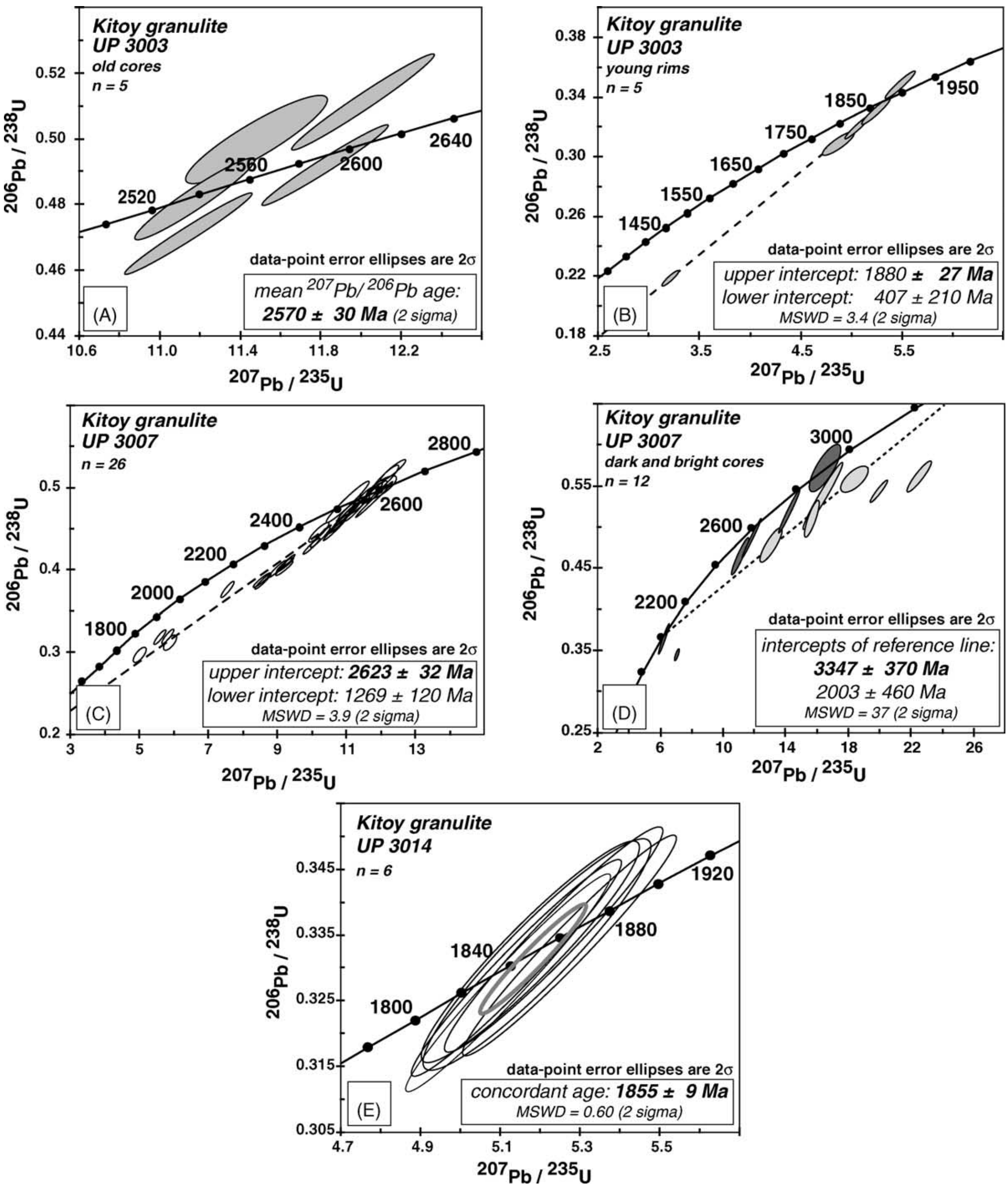

Fig. 2. $^{206}Pb/^{238}U$ vs. $^{207}Pb/^{235}U$ concordia diagrams for Kitoy samples: (A) Kitoy granulite UP 3003: Archean granulite formation. (B) Kitoy granulite UP 3003: First Proterozoic granulite formation. (C) Kitoy granulite UP 3007: Archean granulite formation. (D) Kitoy granulite UP 3007: Archean protolith emplacement. (E) Kitoy granulite UP 3014: Second Proterozoic granulite formation.

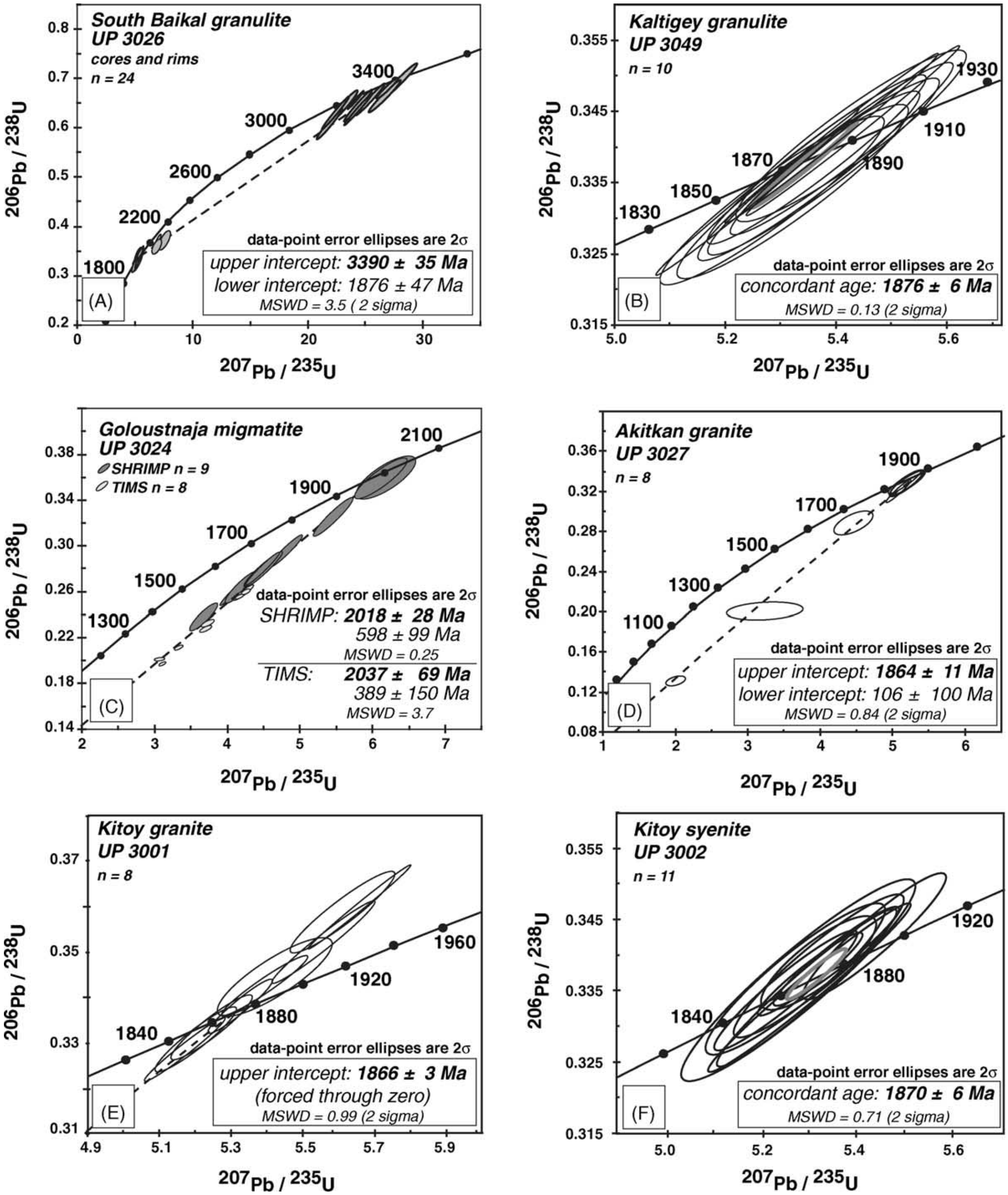

Fig. 3. $^{206}Pb/^{238}U$ vs. $^{207}Pb/^{235}U$ concordia diagrams for Southern Siberian samples: (A) Sharizhalgai granulite UP 3026: Archean protolith emplacement and First Proterozoic granulite formation. (B) Kaltigey granulite UP 3049: First Proterozoic granulite formation. (C) Goloustnaja migmatite UP 3024: Proterozoic migmatisation. (D) Akitkan granite UP 3027: Proterozoic granite emplacement. (E) Kitoy granite UP 3001: Proterozoic granite emplacement. (F) Kitoy syenite UP 3002: Proterozoic granite emplacement.

Five spots representing old cores are defining an Archean age at 2.56 Ga (Fig. 2A). The analysed areas are core regions with very different CL features. Overprinted magmatic zoning is found as well as cloudy diffuse CL of medium intensities. Also a rather weak luminescent interior area (3003-39.1) was measured and resulted in a 2.5 Ga old spot.

Fig. 2B shows the result of the other five analyses: these rim analyses can be combined on a discordia line hitting the concordia at 1.88 Ga (supported by the nearly concordant analyses 3003-54.1 and 3003-50.1) with a lower intercept of 407 ± 210 Ma. Similar Palaeozoic lower intercept ages are reported from this part of Siberia (Poller et al., 2003) and from the Aldan shield (Kotov et al., 1995).

The second granulite sampled at Kitoy area, UP 3007, was mainly dated by SHRIMP RG at ANU and a few additional points were acquired by SHRIMP II at Curtin University. Altogether 38 analyses are presented for this sample in Table 1 and Fig. 2C and D. Again two main ages could be detected by the zircon analyses.

The first group of zircons defines a similar Archean age of 2.6 Ga as in sample UP 3003, (Fig. 2C) based on a somewhat scattered discordia line and concordant analyses. Looking with cathodoluminescence the 2.6 Ga ages are located in outer magmatic zoned areas (e.g. 3007-80.1) with dark luminescence as well as in bright overgrowth rims (e.g. 3007-69.1), dark to grey luminescent cores (e.g. 3007-65.1) and areas with intermediate luminescence in inner and outer areas (e.g. 3007-32.2). Fig. 2D also shows a variety of older inherited cores confirming an Archean emplacement for the precursor. These cores range from very brightly CL with magmatic zoning such as 3007-44.1 or 3007-56.3 to darkly luminescent cores (e.g. 3007-101.1).

The third granulite from Kitoy area, UP 3014 shows a much simpler age spectrum than the two other samples. As presented in Fig. 2E all analysed spots resulted in concordant ages at 1.85 Ga, an age younger than the 1.88 Ga found in UP 3003. The measured zircons of sample 3014 are grey to dark in CL, showing zoned domains as well as cloudy structures, typical for metamorphic growth (Hoskin and Black, 2000; Corfu et al., 2003). However, in age no differences between the magmatically zoned cores and the cloudy overgrowth was found.

The last granulite of Kitoy area (UP 3016) did not contain many zircons. The few grains that could be isolated were rather tiny and difficult to analyse. Table 1 gives the results of the 4 analysed spots. Only one grain (3016-7.1) resulted in a concordant age of 1.84 Ga. Two other zircons showed Palaeoproterozoic ages with recent Pb loss; one inherited Archean grain was also analysed. Due to similarities in geochemical and isotopical composition this sample is regarded to be the same granulite type as UP 3014.

5.2. Kitoy Granites (UP3001, UP3002)

In addition to the granulites also two granites from Kitoy River which were already dated by TIMS (Poller et al., 2004) were also used for SHRIMP zircon analyses (Table 1). Both granitoids are Palaeoproterozoic in age. The zircons of granite UP 3001 (Fig. 3E) were slightly discordant due to Pb loss. However, the upper intercept age of 1866 ± 3 Ma describes the crystallisation age quiet precise. Zircon dating of sample UP 3002, which shows only pure magmatically zoned crystalls, resulted in 11 concordant points with a mean age of 1870 ± 6 Ma (Fig. 3F).

5.3. The South-Baikal Granulite (UP3026)

This granulite sampled along the Transsiberian railway exposed the most spectacular CL images. Almost all investigated grains show very bright luminescent overgrowing areas up to 80 μm wide (e.g. 3026-35, 3026-40). In the inner parts these zircons bear magmatic-zoned cores (e.g. 3026-34, 3026-53), sometimes with dark intermediate zones (e.g. 3026-36, 3026-46) overgrown by bright luminescent rims.

The U–Pb data yield two distinct ages (see Fig. 3A). The first is defined at 3.4 Ga by concordant and slightly discordant analyses measured in the dark luminescent core areas, which often show magmatic features.

The lower intercept age of the discordia line at 1.88 Ga is defined by the bright luminescent rims and some grey luminescent areas. Almost all analysed bright rims are concordant at this Proterozoic age, which is in perfect correspondence with the 1.88 Ga found in UP 3003 at Kitoy (see Fig. 2B).

By contrast, the 2.6 Ga event found at Kitoy area was not detected in the South-Baikal granulite.

The 1.88 Ga age found in the South-Baikal area corroborates the lower intercept ages reported by Aftalion et al. (1991) for high-grade rocks of this outcrop. However, the upper intercept ages of the Aftalion et al. (1991) study (around 2.7 Ga) could not be found.

5.4. Goloustnaja salient: Goloustnaja migmatite (UP 3024)

The Goloustnaja migmatite was dated not only by SHRIMP but also by TIMS.

The analyses (Fig. 3C) are mostly discordant and define overlapping upper intercept ages of 2.02 Ga for the SHRIMP and 2.04 Ga for the TIMS data. Therefore the two techniques are in good correspondence to each other.

All measured zircons are magmatically zoned without any cores or overgrowths but bear many inclusions (mainly apatite). It is obvious that these frequent apatite inclusions, which are between 5 and 20 μm in diameter, are lowering the $^{206}Pb/^{204}Pb$ ratios (see Table 2) and increase the common Pb correction.

5.5. The Primorsk salient: Kaltigey granulite (UP3049)

The zircons of the Kaltigey granulite show no bright rims, but have magmatic core components (bright and dark luminescent), often surrounded by very dark rims.

All analysed spots on rims and cores resulted in concordant ages (Fig. 3B) with a mean age of 1.88 Ga, perfectly fitting the results of the Kitoy and South-Baikal granulites. Archean components were not detected in this sample.

5.6. The Baikal salient: Akitkan granite (UP3027)

Among the granites present along the margin of the Southern Siberian Craton those from the Kitoy area (UP 3001, UP 3002 and UP 3005) were dated by Poller et al. (2004) at 1.88 Ga and 1.85 Ga. A granite from the Akitkan belt, representative for the Northern Baikal area, was included in this study. The zircons of this sample show homogeneous magmatic zoning with grey luminescence. Outer areas appear either bright or dark in CL, but are always magmatically zoned.

The SHRIMP dating of the Akitkan granite UP 3027 resulted in an age of 1.86 Ga (Fig. 3D). Whereas 5 of the spots are concordant, three spots show recent Pb loss indicated by the lower intercept of 106 ± 100 Ma. The Akitkan granite fits well within the timing of Proterozoic granite emplacements along the southern margin of the Siberian Craton.

6. Discussion

The zircon data presented in this study give evidence for a multistage magmatic as well as metamorphic evolution of the southern part of the Siberian Craton. Altogether five different age groups were found, representing different magmatic and/or metamorphic events. Fig. 4 gives an overview to these events and presents also examples of the CL features where the reported ages were found (the black and white ellipses mark the analysed SHRIMP spots).

The oldest detected age was found in two granulites from two different locations of the Sharizhalgai salient. The acidic Kitoy granulite (UP 3007) and the South-Baikal granulite (UP 3026) show both an Archean age around 3.4 Ga. Especially for the South-Baikal granulite the dating resulted in a rather good defined Archean age, measured on dark luminescent cores. These cores all show magmatic zoning and most of them are concordant. Therefore, this age is interpreted to reflect the emplacement of the magmatic precursor of this granulite.

For the Kitoy sample UP 3007 the Archean age is less good defined, but nevertheless all presented Archean ages are also found on magmatic-zoned zircon areas. Consequently the intrusion of a magmatic precursor already in Archean times is not only limited to one outcrop, but is detected in the Sharizhalgai salient in the Kitoy and the South-Baikal areas.

The metamorphic history of the investigated granulites starts also in Archean times. The 2.6 Ga event found in the Kitoy samples UP 3003 and UP 3007 documents a first granulite metamorphism at this time. The fact that this age was measured in dark luminescent rims as well as in bright luminescent cloudy and diffuse appearing zones confirms that the responsible event must be a metamorphic one otherwise the cloudy structures would not be present (Corfu et al., 2003). The 2.6 Ga overprinting seems to be the major metamorphic event at least for the UP 3007 sample, in which no significant younger overprint was found. In contrast UP

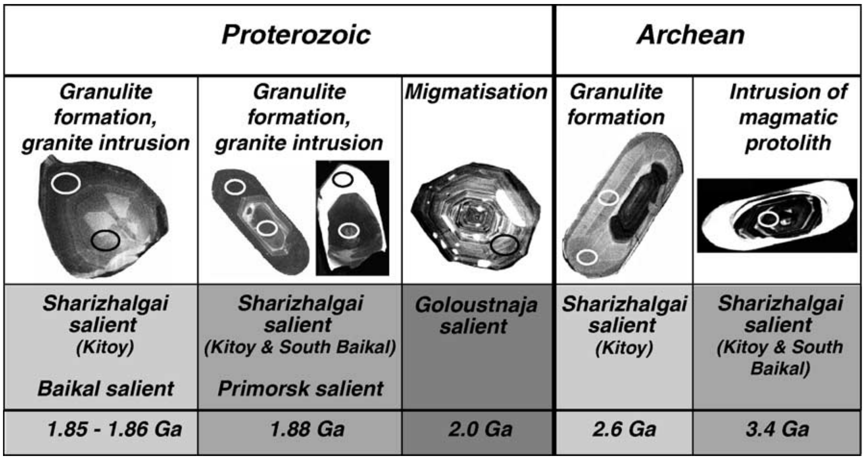

Fig. 4. Summary of the age stages along the margin of the Southern Siberian Craton. The ellipses in the CL images mark the spots where the ages reported in this figure were measured.

3003 shows a second Proterozoic zircon component. The absence of this age in UP 3007 suggests that these two granulites may have been situated in two different crustal levels during Archean/Proterozoic times.

The next younger event at 2.0 Ga is absent in the granulitic rocks, but present in the Goloustnaja migmatite UP 3024 (Fig. 3C). The perfect magmatic zones visible under CL show no overprinting at all, and are therefore interpreted as a result of a high temperature melting during migmatisation. The growth of such magmatically zoned zircons during migmatitic stages are known also from other orogenic areas (Poller and Todt, 2000).

The most frequently found age is the 1.88 Ga event, detected in the Kitoy granulite UP 3003, the South-Baikal granulite UP 3026 (both from the Sharizhalgai salient) and the Kaltigey granulite UP 3049 (the Primorsk salient). Additionally this age was found in the Kitoy granites UP 3001 and UP 3005 (see Table 2 and Poller et al., 2004). This major geological event, which has influenced nearly the whole southern margin of the Siberian Craton, is interpreted as granite emplacement and granulite formation.

Due to the affinity of the investigated granites towards collisional granitoids, this combined magmatic and metamorphic Early Proterozoic stage is most probably connected to an early collision of not yet defined microplates contributing to the amalgamation of the Siberian Craton. Such a process could be responsible first for the high temperature granulite formation connected to the accretion process and later for the intrusion of granitic magmas.

The next step in the large-scale tectonic evolution of the Siberian Craton amalgamation at 1.85–1.86 Ga involved granulite formation (UP 3014, Kitoy area) and granite emplacement (e.g. Akitkan granite UP 3027 or Holomha two mica granite UP 3023, see Poller et al., 2004). The collision of microplates was probably connected to underplating and crustal thickening, possibly responsible for a high-grade metamorphic overprint and a second generation of Early Proterozoic granulites. In contrast to the older ones, the 1.85 Ga granulites are significantly mafic with very low SiO_2 content and seem to have been generated from a different source than the 1.88 Ga old granulites.

The fact, that the zircons and also the common Pb system (Poller et al., 2004) were not disturbed after 1.85 Ga gives evidence that the amalgamation of the Siberian Craton must have been completed in the Palaeoproterozoic. An additional argument for the constitution of the Siberian Craton already in Early Proterozoic times is the 1963 ± 163 Ma age of the Rb–Sr errorchrone of Aftalion et al. (1991) for a garnet bearing gneiss of the Sharizhalgai salient that is in good correspondence to our 1.88 Ga zircon age for granulite metamorphism. Therefore, these crystalline rocks record no significantly younger geological process, such as the assemblage of the Rodinia supercontinent around 1.4 Ga ago. It appears that the southern margin of the craton was screened from these processes because it was already part of a larger continental block.

Besides the evolution of the Siberian Craton also an other general geodynamic implication has to be considered. The main magmatic and metamorphic events which were detected in the Siberian granites and granulites are those between 1.88 and 1.85 Ga. This time span is equal to the main peak of continental growth and the initial stage of supercontinent formation in the Palaeoproterozoic (Condie, 2000, 2002). The study of Condie (2002) is based on data from Laurentia, Baltica, Australia and Africa but did not include data from Siberia due to the lack of ages. According to new geochronological data the time array for a Palaeoproterozoic supercontinent assembly exactly overlaps the stages detected along the Southern Siberian Craton.

Zhao et al. (2002) discuss a large amount of data from Early Proterozoic orogens including nearly all continental masses. Siberia is represented only by data from the Aldan shield and the Stanovoy Belt (Nutman et al., 1992; Rosen et al., 1994). Few data from the Akitkan belt (Rosen et al., 1994; Condie and Rosen, 1994) are also discussed as possible Proterozoic collisional belt. The main conclusion of Zhao et al. (2002) is the possible existence of a pre-Rodinia supercontinent, called Columbia by Rogers and Santosh (2002). The presented age data from the southern margin of the Siberian Craton fit with this idea of an Early Proterozoic supercontinent. Our data imply that the Siberian Craton was being amalgamated at this time.

7. Summary

This geochronological study gives evidence for a multistage evolution of the Siberian Craton. It starts with an Archean precursor and includes one Archean and two Palaeoproterozoic granulite formations. Additionally a Proterozoic migmatisation event and two stages of granite emplacement along the margin of the Craton were documented to have happened in Palaeoproterozoic. These main events mark the amalgamation of the Siberian Craton and give further hints for the participation of the Siberian Craton during the formation of Columbia.

Acknowledgements

We are grateful to J. Huth for his help at the scanning electron microscope and the CL. Mark Fanning, Robert Pidgeon and Adam Frew are greatly acknowledged for their help at the SHRIMP at ANU and Curtin University of Technology. We thank A. Hofmann for the opportunity to perform this study at MPI. This work was supported by the DFG (PO 608/4-1 and PO 608/3-2), Russian Foundation for Basic Research (#04-05-64412) and by Russian Science Support Foundation. Helpful remarks and review comments by J.W. Rogers and F. Corfu are greatly acknowledged.

References

Aftalion, M., Bibikova, E.V., Bowes, D.R., Hopgood, A.M., Perchuk, L.L., 1991. Timing of early Proterozoic collisional and extensional events in the granulite–gneiss–charnokite–granite complex, Lake Baikal, USSR: A U–Pb, Rb–Sr and Sm–Nd isotopic study. J. Geol. 99, 851–862.

Compston, W., Williams, I.S., Meyer, C., 1984. U–Pb geochronology of zircons from lunar breccia73217 using a sensitive high mass-resolution ion microprobe. J. Geophys. Res. 89 (Suppl.), B525–B534.

Condie, K.C., 2000. Episodic continental growth and supercontinents: a mantle avalanche connection? Earth Planet. Sci. Lett. 163, 97–108.

Condie, K.C., 2002. Continental growth during a 1.9 Ga superplume event. J. Geodyn. 34, 249–264.

Condie, K.C., Rosen, O.M., 1994. Laurentia—Siberia connection revisited. Geology 22, 168–170.

Corfu, F., Hanchar, J.M., Hoskin, P.W.O., Kinny, P., 2003. Atlas of Zircon Textures. In: Hanchar, J.M., Hoskin, P.W.O. (Eds.), Zircon. Reviews in Mineralogy & Geochemistry, vol. 53, pp. 469–500.

Donskaya, T.V., Salnikova, E.B., Sklyarov, E.V., Gladkochub, D.P., Mazukabzov, A.M., Kovach, V.P., Yakovleva, S.Z., Berezhnaya, N.G., 2002. Early proterozoic postcollisional magmatism at the southern flank of the Siberian Craton: new geochronological data and geodynamic implications. Doklady Earth Sci. 383 (2), 125–128.

Donskaya, T.V., Bibikova, E.V., Mazukabzov, A.M., Kozakov, I.K., Gladkochub, D.P., Kirnozova, T.I., Plotkina, Yu.V., Reznitsky, L.Z., 2003. The Primorsk granitoid complex of western Cisbaikalia: geochronology and geodynamic typification. Russ. Geol. Geophys. (Geologia i Geofizika) 44 (10), 968–979.

Gladkochub, D.P., Sklyarov, E.V., Donskaya, T.V., Mazukabzov, A.M., 2003. Not complete break-up of a Palaeoproterozoic supercontinent: evidence from South Siberia. Geophys. Res. Abstr. 5, 00616.

Gladkochub, D.P., Donskaya, T.V., Mazukabzov, A.M., Salnikova, E.B., Sklyarov, E.V., Yakovleva, S.Z., 2005. Kitoy granite complex (southern part of the Siberian Craton): composition, age, geodynamic setting. Russ. Geol. Geophys. (Geologia i Geofizika), in press.

Hoskin, P.W.O., Black, L.P., 2000. Metamorphic zircon formation by solid-state recrystallization of protolith igneous zircon. J. Metamorph. Geol. 18, 423–439.

Kotov, A.B., Kovach, V.P., Salnikova, E.B., Glebovitskii, V.A., Yakovleva, S.Z., Berezhnaya, N.G., Myskova, T.A., 1995. Continental crustal age and formation stages in the Central Aldan Granulite-Gneiss Terrain: U–Pb and Sm–Nd isotopic data for granitoids. Petrology 3, 87–97.

Krogh, T.E., 1973. A low-contamination method for hydrothermal decomposition of zircon and extraction of U and Pb for isotopic age determinations. Geochim. Cosmochim. Acta 37, 485–494.

Larin, A.M., Salnikova, E.B., Kotov, A.B., Kovalenko, V.I., Rytsk, E. Yu., Yakovleva, S.Z., Berezhnaya, N.G., Kovach, V.P., Buldygerov, V.V., Sryvtsev, N.A., 2003. The North Baikal Volcanoplutonic belt: age, formation duration, and tectonic setting. Doklady Earth Sci. 392 (7), 963–967.

Levitskii, V.I., Mel'nikov, A.I., Reznitskii, L.S., Bibikova, E.V., Kirnozova, T.I., Kozakov, I.K., Makarov, V.A., Plotkina, Yu.V., 2002. Early Proterozoic postcollisional granitoids in southwestern Siberian Platform. Russ. Geol. Geophys. (Geologia i Geofizika) 43 (8), 679–692.

Ludwig, K., 1999. Using Isoplot/Ex, Version 2.01: A Geochronological Toolkit for Microsoft Excel. Berkeley Geochronology Center Special Publication, vol. 1a: 47.

Ludwig, K., 2001. Squid 1.02—A User's Manual. Berkeley Geochronology Center Special Publication, vol. 2, 19 pp.

Nutman, A.P., Chernyshev, I.V., Baadsgaard, H., Smelov, A.P., 1992. The Aldan Shield of Siberia, USSR: the age of its Archean components and evidence for widespread reworking in the mid-Proterozoic. Precambr. Res. 54, 195–210.

Poller, U., 2000. A combination of single zircon dating by TIMS and cathodoluminescence investigations on the same grain: The CLC-method—U–Pb geochronology for metamorphic rocks. In: Pagel, M., Barbin, V., Blanc, Ph., Ohnenstetter, D. (Eds.), Cathodoluminescence in Geosciences. Springer-Verlag, Heidelberg, Berlin, pp. 401–414.

Poller, U., Todt, W., 2000. U–Pb single zircon data of granitoids from the High Tatra Mountains (Slovakia): implications for the geodynamic evolution. Transactions of Royal Society of Edinburgh. Earth Sci. 91, 235–243.

Poller, U., Gladkochub, D., Donskaya, T., Mazukabzov, A., Sklyarov, E., Todt, W., 2003. New geochronological and isotopical data imply early Proterozoic assembling of the southern Siberian Craton. Hutton Symposium V: The Origin of Granites and Related Rocks. Geological Survey of Japan, Interim Report 29, 120.

Poller, U., Gladkochub, D., Donskaya, T., Mazukabzov, A., Sklyarov, E., Todt, W., 2004. Early Proterozoic collisional magmatism along the Southern Siberian Craton—constrains from U–Pb single zircon data. Transactions of Royal Society, Edinburgh, Earth Sciences, 95 (Hutton V volume).

Rogers, J.J.W., Santosh, M., 2002. Configuration of Columbia, a Mesoproterozoic supercontinent. J. Geol. 104, 91–107.

Rosen, O.M., Condie, K.C., Natapov, L.M., Nozhkin, A.D., 1994. Archean and Early Proterozoic evolution of the Siberian Craton: a preliminary assessment. In: Condie, K.C. (Ed.), Archean Crustal Evolution. Elsevier, Amsterdam, pp. 411–459.

Todt, W., Cliff, R.A., Hanser, A., Hofmann, A.W., 1996. Evaluation of a ^{202}Pb–^{205}Pb double Spike for high-precision lead isotope analysis. In: Geophysical Monograph, vol. 95. American Geophysical Union, pp. 429–437.

Williams, I., 1998. U–Th–Pb geochronology by ion-microprobe. In: McKibben, M.A., Shanks III, W.C., Ridley, W.I. (Eds.), Applications of Microanalytical Techniques to Understanding Mineralizing Processes. In: Reviews in Economic Geology, vol. 7. pp. 1–35.

Zhao, G., Cawood, P.A., Wilde, S.A., Sun, M., 2002. Review of global 2.1–1.8 Ga orogens: implications for a pre-Rodinia supercontinent. Earth Sci. Rev. 59, 125–162.